Rhizobial peptidase HrrP cleaves host-encoded signaling peptides and mediates symbiotic compatibility

Paul A. Price[a], Houston R. Tanner[a], Brett A. Dillon[a], Mohammed Shabab[b], Graham C. Walker[b], and Joel S. Griffitts[a,1]

[a]Department of Microbiology and Molecular Biology, Brigham Young University, Provo, UT 84602; and [b]Department of Biology, Massachusetts Institute of Technology, Cambridge, MA 02139

Edited by Eva Kondorosi, Hungarian Academy of Sciences, Biological Research Centre, Szeged, Hungary, and approved May 27, 2015 (received for review September 15, 2014)

Legume–rhizobium pairs are often observed that produce symbiotic root nodules but fail to fix nitrogen. Using the *Sinorhizobium meliloti* and *Medicago truncatula* symbiotic system, we previously described several naturally occurring accessory plasmids capable of disrupting the late stages of nodule development while enhancing bacterial proliferation within the nodule. We report here that host range restriction peptidase (*hrrP*), a gene found on one of these plasmids, is capable of conferring both these properties. *hrrP* encodes an M16A family metallopeptidase whose catalytic activity is required for these symbiotic effects. The ability of *hrrP* to suppress nitrogen fixation is conditioned upon the genotypes of both the host plant and the *hrrP*-expressing rhizobial strain, suggesting its involvement in symbiotic communication. Purified HrrP protein is capable of degrading a range of nodule-specific cysteine-rich (NCR) peptides encoded by *M. truncatula*. NCR peptides are crucial signals used by *M. truncatula* for inducing and maintaining rhizobial differentiation within nodules, as demonstrated in the accompanying article [Horváth B, et al. (2015) *Proc Natl Acad Sci USA*, 10.1073/pnas.1500777112]. The expression pattern of *hrrP* and its effects on rhizobial morphology are consistent with the NCR peptide cleavage model. This work points to a symbiotic dialogue involving a complex ensemble of host-derived signaling peptides and bacterial modifier enzymes capable of adjusting signal strength, sometimes with exploitative outcomes.

symbiosis | nitrogen fixation | metallopeptidase | NCR peptides

Plants have a fundamental dependence on nitrogen as a macronutrient, but the vast supply of diatomic nitrogen in the atmosphere is not directly available to plants. Various species of nitrogen-fixing bacteria (collectively known as "rhizobia") form symbiotic associations with grain and forage legumes to produce biologically available nitrogen. Free-living rhizobia recognize potential legume nodulation partners through a highly specific chemical dialogue involving the secretion and perception of the small-molecule signaling compound known as "nodulation (Nod) factor." Recognition of Nod factor by the plant host initiates nodule development, starting with the proliferation of root cortical cells to produce nodule tissue and the formation of microscopic tubules (infection threads) through which trapped rhizobia grow into the expanding nodule tissue. A large fraction of the nodule cells becomes competent to take up the incoming bacteria via endocytosis. Internalized rhizobia (termed "bacteroids") occupy host cells at high density while remaining encased in host-derived symbiosome membranes. Nascent symbiosomes with enclosed bacteroids then undergo a precisely controlled developmental program, becoming large organelle-like structures that are capable of nitrogen fixation (1).

In a subset of legumes, bacteroid development involves an arrest in cell division, genomic endoreduplication, and a 5- to10-fold increase in bacteroid size, resulting in swelled bacteroids that fix copious amounts of nitrogen and are terminally differentiated (2). This is the case for the well-characterized symbiosis between *Sinorhizobium meliloti* and its legume host *Medicago truncatula*. Legumes that induce bacteroid swelling and terminal differentiation also encode complex assortments of nodule-specific cysteine-rich (NCR) peptides that are specifically expressed in nodules and are delivered to the bacteroid-containing symbiosomes, suggesting a peptide-based mechanism for bacteroid development that is under strict host control (3–5). *M. truncatula* encodes ~600 distinct NCR peptides that are expressed in at least two waves during nodule development (6–8). These peptides are generally 30–60 amino acids in length and share little sequence similarity with one another, except for the presence of four to six cysteine residues that are thought to form intramolecular disulfide bridges (9). When applied to free-living rhizobia in vitro, certain synthetic NCR peptides are sufficient to cause many of the metabolic and morphological changes observed for bacteroids *in planta* (5, 10). As the accompanying article (11) details the first strong genetic evidence, to our knowledge, a specific NCR peptide (NCR169) plays a decisive role in bacteroid development in *M. truncatula* nodules. It currently is supposed that the in vivo deployment of NCR peptides to bacteroid-containing symbiosomes is optimized to bring about cell division arrest, genomic endoreduplication, cell enlargement, and gentle membrane permeabilization while maintaining the robust metabolic activity required for nitrogen fixation and nutrient exchange with the host.

We previously described several naturally occurring *Sinorhizobium* accessory plasmids (pHRs) capable of restricting nodule development and nitrogen fixation (12). This effect is host dependent, with pHR plasmids causing dramatic symbiotic defects on certain *Medicago* host species but having no effect on others. We report here that a pHR-encoded metallopeptidase modulates symbiotic outcomes at a late developmental stage by triggering the premature degeneration of differentiated bacteroids, concomitant with nodule senescence in some cases. This enzyme is capable of NCR peptide cleavage in vitro, and its expression

Significance

The agriculturally important symbiosis between nitrogen-fixing bacteria (rhizobia) and their legume hosts occurs within root nodules. This partnership requires a molecular dialogue that ensures specificity and directs the codevelopment of the two organisms during nodule formation. This paper characterizes a protein, host range restriction peptidase (HrrP), which plays a role in this dialogue. Rhizobial strains that express HrrP tend to exhibit more parasitic properties, such as failing to provide fixed nitrogen for their hosts and proliferating more abundantly within nodule tissue. HrrP likely exhibits these properties by actively degrading plant-derived chemical signals that normally stimulate symbiotic cooperation.

Author contributions: P.A.P., G.C.W., and J.S.G. designed research; P.A.P., H.R.T., and B.A.D. performed research; M.S. directed experiments; G.C.W. and J.S.G. supervised the research; M.S. contributed new reagents/analytic tools; P.A.P. analyzed data; and P.A.P. and J.S.G. wrote the paper.

The authors declare no conflict of interest.

This article is a PNAS Direct Submission.

Data deposition: The sequence reported in this paper has been deposited in the GenBank database (accession no. CP011000).

[1]To whom correspondence should be addressed. Email: joelg@byu.edu.

This article contains supporting information online at www.pnas.org/lookup/suppl/doi:10.1073/pnas.1417797112/-/DCSupplemental.

pattern is consistent with a role in modifying NCR peptide pools in nodule tissue.

Results

Identification of Host Range Restriction Peptidase as a Nitrogen-Fixation Blocking Factor. We have previously shown that *S. meliloti* strain B800 (a streptomycin-resistant derivative of USDA1963) is able to fix nitrogen (Fix^+) on *M. truncatula* accession A17 but not on accession A20 (Fix^-) and that nitrogen fixation is restored upon spontaneous curing of its accessory plasmid, pHRB800 (12). This large (199-kb) plasmid contains ∼290 protein-coding genes and is able to confer a Fix^- phenotype when present in multiple *S. meliloti* strain backgrounds. To determine which part of this plasmid is responsible for the Fix^- phenotype, a saturating plasmid-specific transposon mutagenesis screen was carried out on pHRB800, and this mutant library was screened for the inability to induce a Fix^- phenotype on A20 plants (outlined in Fig. S1). Five pHRB800 transposon insertions that prevented the fixation-blocking phenotype all mapped to a single gene encoding an M16A family zinc-metallopeptidase, hereafter designated "host range restriction peptidase" (*hrrP*).

As expected, targeted disruptions of *hrrP* also yield a Fix^+ phenotype on accession A20 (Fig. S2). When the *hrrP* gene is placed on a small plasmid vector and moved into a pHR-cured (pHR^-) version of strain B800, the Fix^- phenotype is restored as though pHRB800 were present. Placement of *hrrP* onto the chromosome (*hrrP*_chr) of B800 pHR^- using a mini-Tn*5* transposon vector also restores the fixation-blocking phenotype on A20, mimicking the behavior of pHRB800 (Fig. 1*A*). Indeed, chromosomal *hrrP* has a more complete fixation-blocking effect, presumably because the chromosome, unlike a plasmid, cannot be cured during symbiotic invasion of the nodule. Notably, *hrrP* does not appear to affect nitrogen fixation on accession A17 (Fig. 1*B*). Acetylene reduction assays, which directly measure nitrogenase activity, reveal that *hrrP* inhibits activity on *M. truncatula* A20 almost completely but has no effect on A17 (Fig. 1*C* and Figs. S2*C* and S3). The lack of nitrogen fixation is also evident in the reduced shoot dry weight and yellowing chlorotic leaves of plants grown under nitrogen-limiting conditions (Fig. 1 *A* and *D*). Together these results show that *hrrP* is necessary and sufficient for host-specific inhibition of nitrogen fixation.

The M16A metallopeptidase family is characterized by a highly conserved HxxEH structural motif that coordinates the active-site Zn^{2+} ion. To determine whether the proteolytic function of HrrP is necessary for is its fixation-blocking phenotype, we introduced an E62A (HxxEH→HxxAH) alteration that is predicted to disable the peptidase catalytic motif. This variant no longer blocks nitrogen fixation (Fig. 1 *A*, *C*, and *D*), indicating that the peptidase activity of HrrP is responsible for the fixation-blocking phenotype.

The Symbiotic Effects of *hrrP* Are Conditioned by both Host and Strain Genetic Background. It is clear that *hrrP* distinguishes *M. truncatula* accessions A20 and A17 when in the *S. meliloti* B800 strain background (Fig. 1). Fig. 2*A* shows that on a larger panel of *M. truncatula* accessions *hrrP* exhibits a broad spectrum of symbiotic effects (Fig. S4). These effects range from unimpeded nitrogenase activity (A17, L000163, L000174, and L000542) to nearly complete elimination of nitrogen fixation (A20 and L000239). Therefore, different closely related legume hosts, all of which form infected nodules, exhibit differing responses to rhizobially expressed *hrrP*.

hrrP also can have differing effects on host responses, depending on which rhizobial strain is expressing it. For example, *hrrP* expressed in *S. meliloti* strain B800 blocks nitrogen fixation on *M. truncatula* A20 but not on A17, whereas *hrrP* expressed in *S. meliloti* strain B464 blocks nitrogen fixation on both A20 and A17. Such variation in strain range can be observed for diverse *Sinorhizobium* isolates (Fig. 2*B*, Fig. S5, and Table S1). The strain-range effect demonstrates the existence of rhizobial genes that act as modifiers of the *hrrP*-induced fixation-blocking phenotype. In an attempt to identify the gene(s) that modulate strain range, we performed saturating transposon mutagenesis on B800 pHR^- *hrrP*_chr, followed by a screen for Fix^+ nodules on A20 (i.e., suppressors of the Fix^- phenotype). This screen yielded eight Fix^+ nodules; however, each of these strains had independent transposon insertions in *hrrP* itself. Our inability to uncover an *hrrP*-modifying function in this simple manner suggests that the unknown function either is essential for nitrogen fixation or is distributed over multiple overlapping functions.

***hrrP* Transcription Is Nodule Specific and Not Host Conditioned.** To evaluate *hrrP* gene expression in the nodule, transcriptional fusions to β-glucuronidase (GUS) were constructed in a manner that would not disrupt normal *hrrP* function. Similar fusions also were made to the *nifHDK* nitrogenase promoter (normally up-regulated in the nodule) and the *flaB* flagellin promoter [normally down-regulated in the nodule (13)]. All reporter strains carried pHRB800, and nodules were stained at 10 d postinoculation (dpi) to capture events before major morphological differences between Fix^- and Fix^+ nodules are evident. We observed strong *hrrP*-GUS staining in nodules in both A17 and A20 host plants (Fig. 3 *A* and *B*). The *hrrP*-GUS expression pattern overlaps with that of *nifH*-GUS, with staining evident throughout the zones of the nodule that ordinarily are occupied by developing and mature bacteroids. Remarkably, *hrrP* transcription in the nodule does not appear to interfere with *nif* gene expression, even in A20 where *hrrP*

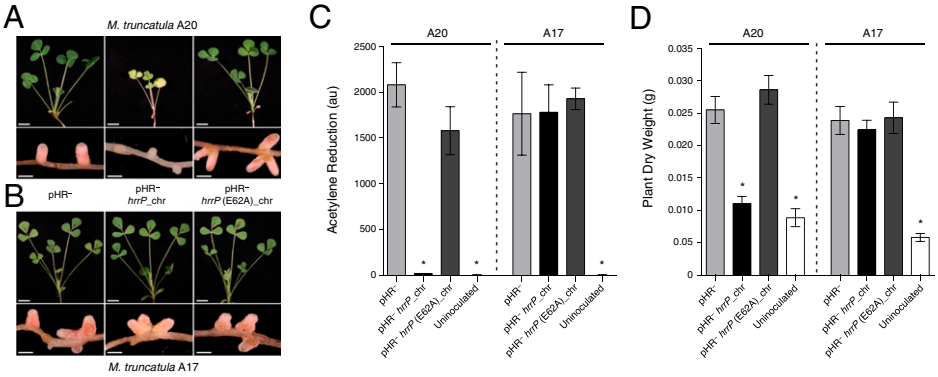

Fig. 1. *hrrP* is necessary and sufficient to inhibit nitrogen fixation on *M. truncatula* accession A20 but not A17. (*A* and *B*) Images of shoots and nodules at 28 dpi of *M. truncatula* A20 (*A*) and A17 (*B*) induced with strains B800 pHR^- (plasmid-cured derivative of B800; C307), B800 pHR^- with a chromosomal copy of *hrrP* (PP317), or B800 pHR^- with a chromosomal copy of *hrrP*(E62A) (PP316). (*C* and *D*) Acetylene reduction data at 21 dpi ($n = 4$) (*C*) and plant shoot dry weight data at 28 dpi ($n = 5$) (*D*) for *M. truncatula* A20 and A17 plants inoculated with these same *Sinorhizobium* strains. (Scale bars: shoots, 1 cm; nodules, 0.1 cm.) Error bars indicate SEM. *$P < 0.0001$ for Student's *t* test vs. strain B800 pHR^-.

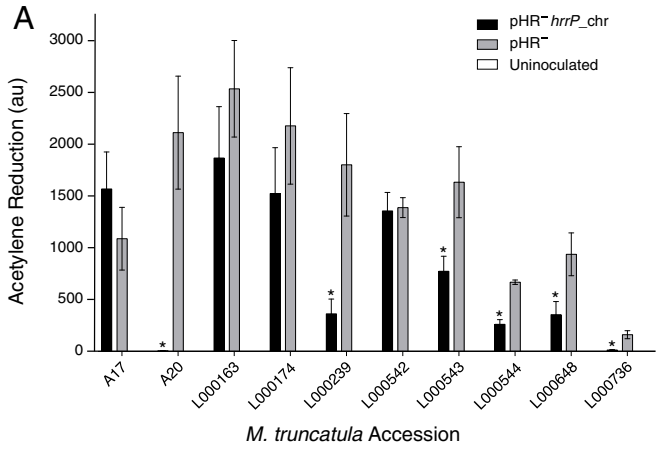

B

	M.t. A17		M.t. A20	
Strain	WT	hrrP _chr	WT	hrrP_chr
B641	Fix +	Fix +	Fix +	Fix +
B644	Fix +	Fix +	Fix +	Fix +
C285	Fix +	Fix +	Fix +	Fix −
B800 pHR⁻	Fix +	Fix +	Fix +	Fix −
B464	Fix +	Fix −	Fix +	Fix −
B475	Fix +	Fix −	Fix +	Fix −

Fig. 2. The symbiotic effects of *hrrP* are conditioned by both host and strain genetic backgrounds. (*A*) Acetylene reduction data ($n = 3$) for a panel of wild *M. truncatula* accessions inoculated with B800 pHR⁻ (C307), B800 pHR⁻ with a chromosomal copy of *hrrP* (PP317), or dH_2O (uninoculated). Error bars indicate SEM. *$P < 0.05$. (*B*) Phenotypic outcomes [Fix⁺ (pink shading) and Fix⁻ (white shading)] for *M. truncatula* A17 and A20 inoculated with *Sinorhizobium* strains B641, B644, C285, B800 pHR⁻ (C307), B464, and B475 with and without a chromosomal *hrrP* transgene ($n = 8$).

evokes a Fix⁻ phenotype. Because *nif* gene expression requires a microaerophilic environment, this observation implies that the early stages of nodule development required to create such an environment are not perturbed by *hrrP* function. In free-living cells, *hrrP*-GUS expression is nearly undetectable compared with expression from the *flaB* promoter or the commonly used *trp* promoter from *Salmonella*, which is constitutive in *S. meliloti* (Fig. 3*C*).

HrrP Cleaves NCR Peptides in Vitro. The observations described above are consistent with the HrrP peptidase acting on host-encoded NCR peptides in the nodule to modulate symbiotic development. Fig. 4*A* depicts a structural model for the HrrP enzyme based on crystallographically determined M16A metallopeptidase family members. The predicted clamshell structure of HrrP is reminiscent of previously solved enzymes, which are known to select peptide substrates based on their ability to be accommodated in the interior of the proteolytic chamber formed by the two roughly symmetrical domains. Substrate size and charge, rather than sequence, seems to be a key determinant of proteolytic specificity within this family (14). The peptide size range accommodated by M16A enzymes (30–70 residues) is remarkably similar to the range of sizes predicted for mature NCR peptides (30–60 residues), leading us to believe that HrrP may act on a large subset of NCR peptides despite their extensive sequence diversity.

To test the NCR peptide cleavage model directly, HrrP and the catalytically inactivated variant HrrP(E62A) were purified to homogeneity, and these preparations were used to treat various purified NCR peptides. Evaluating degradation by gel electrophoresis (Fig. 4*B*) allows the direct observation of NCR079 degradation over a 90-min period in the presence of HrrP that is not observed in the presence of HrrP(E62A). The more limited degradation of NCR129 by HrrP over the same time period suggests some level of NCR peptide substrate selectivity. Time-course analysis of NCR079 degradation by HPLC shows the formation of discrete product peaks during the course of the reaction. Two minor peaks, eluting around 11.5 min and 12.1 min, accumulate during intermediate time points and then diminish in the final time point, suggesting that substrate peptides may be degraded in multiple steps (Fig. 4*C*). HrrP activity on 10 NCR peptides is quantified in Table 1. Degradation is detected for all NCR peptides tested, but activity varies by up to 15-fold. HrrP is modestly active in vitro against NCR169, a peptide reported in the accompanying article (11) as being required for bacteroid development.

***hrrP* Increases *Sinorhizobium* Fitness Within Nodules.** Previous work with pHR plasmids indicated that they can increase bacterial proliferation inside the nodule (12). To test whether *hrrP* can confer this effect and to evaluate whether this property also might be host conditioned, cfus were quantified from individual 28-d-old, surface-sterilized nodules. For A20, *hrrP*⁺ (Fix⁻) nodules yielded 5.5-fold more cfus than *hrrP*⁻ (Fix⁺) nodules (Fig. 5*A*). This finding is striking, considering the small size of the nonfixing *hrrP*⁺ nodules compared with the well-developed *hrrP*⁻ nodules (Fig. 1*A*). Given that the *hrrP*⁺ strain induces 5–10 times more nodules on A20 than the *hrrP*⁻ strain, the effective gain in bacterial proliferation by the *hrrP*⁺ strain on a per-plant basis is ~30-fold. Remarkably, *hrrP* confers a similar fitness benefit in association with accession A17 (a 4.5-fold increase in cfus per nodule), a host background in which *hrrP* does not interfere with nitrogen fixation (Fig. 5*A*).

We tested the idea that the hyperproliferation of *hrrP*⁺ strains in nodules may correspond to the induction of nodule senescence because a senescing nodule may support enhanced saprophytic growth of undifferentiated bacteria. Two expression markers associated with nodule senescence in *M. truncatula* have been

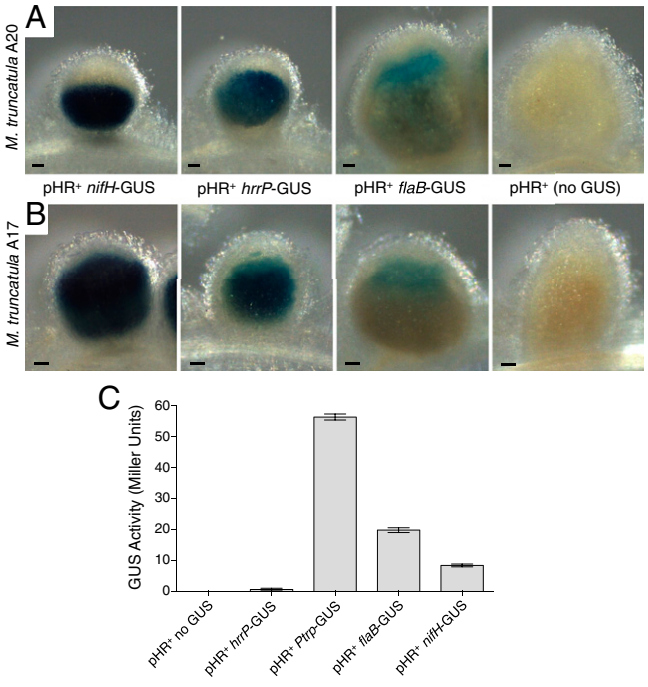

Fig. 3. GUS promoter fusion studies showing nodule-specific expression of *hrrP*. (*A* and *B*) Representative micrographs of 10-d-old *M. truncatula* accession A20 (*A*) and A17 (*B*) nodules stained with X-GLUC to reveal the location and relative expression of the GUS reporter fusions integrated downstream of the *nifHDK*, *hrrP*, and *flaB* promoters (strains PP404, PP389, and PP397, respectively). All samples were stained under identical conditions. Wild-type B800 (no GUS) was used as a negative control for GUS straining *in planta*. (*C*) GUS expression levels in free-living cells grown to midlog phase. The constitutive *Salmonella*-derived *trp* promoter was included as a positive control (PP471). (Scale bars: 100 μm.) Error bars indicate SEM.

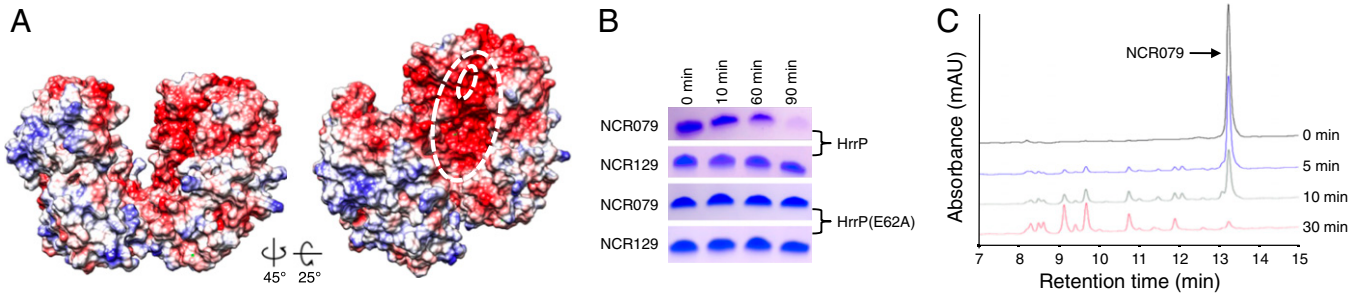

Fig. 4. Purified HrrP cleaves synthetic NCR peptides. (*A*) Electrostatic map of the structural model of HrrP derived using I-TASSER online (closest threading model was PDB ID code 1bccA). The outer white dotted line indicates the catalytic chamber, and the inner white dotted line indicates the Zn^{2+} coordinating residues. (*B*) Tris-Tricine SDS/PAGE gels showing the time course of NCR079 and NCR129 peptide cleavage by purified HrrP or HrrP (E62A). (*C*) HPLC analysis of NCR079 cleavage over time (0, 5, 10, and 30 min) by HrrP.

evaluated recently: *MtCP6*, which encodes a papain-like proteolytic enzyme, and *MtVPE*, which encodes a caspase-like enzyme (15). At 21 dpi, we find that these markers are induced in A20 plants inoculated with *hrrP*$^+$ rhizobia but not A17 plants inoculated with the same strain (Fig. 5*B*). Because both plant genotypes permit the *hrrP*-dependent hyperproliferation phenotype, but only A20 exhibits *hrrP*-dependent senescence, we conclude that senescence may not completely explain the proliferation phenomenon. As expected, A20 and A17 nodules exhibit senescence marker induction when nodulated with nitrogenase-null (Δ*nifH*) rhizobia.

Because the HrrP enzyme cleaves the very peptides that are known to drive bacteroid development, it is tempting to speculate that the enhanced bacterial viability observed in *hrrP*$^+$ nodules is caused by a subset of bacteroids either failing to terminally differentiate or experiencing some sort of dedifferentiation. To begin to explore this hypothesis, we imaged *hrrP*$^+$ bacteroids from A20 nodules by transmission electron microscopy. In *M. truncatula*, the temporal pattern of bacteroid development can be followed indirectly by moving spatially down a single nodule from its meristematic apex to the older, root-proximal zone. For the experiment shown in Fig. 5 *C–F*, an A20 nodule infected with B800 *hrrP*$^+$ bacteria was allowed to develop for 28 d before sample preparation. In the middle region of the nodule (Fig. 5*C*) bacteroids are swollen and elongated, as is typical; in sections taken from the same nodule but closer to the root, bacteroids that normally would maintain their swollen, elongated structure appear to pinch and fragment, resulting in large spaces separating the symbiosome membrane from the bacteroid (Fig. 5 *D–F*). In the most root-proximal region of the nodule bacteroids are small and round (Fig. 5*F*). These degenerative events are not observed in nodules from A17 plants or in newer nodules from A20 plants. The cellular processes that account for this phenomenon are currently under investigation.

Table 1. Specific activity of HrrP against various synthetic NCR peptides

Peptide	Length, aa	pI	HrrP-specific activity, nmol peptide·mg HrrP^{-1}·min^{-1}
NCR035	37	9.44	57.13 ± 4.59
NCR041	31	9.44	52.69 ± 1.27
NCR079	33	6.77	70.16 ± 6.36
NCR094	39	6.21	4.99 ± 1.16
NCR124	30	6.92	14.81 ± 3.38
NCR129	30	4.68	17.15 ± 0.62
NCR142	29	4.01	4.61 ± 3.28
NCR169	38	8.45	10.23 ± 0.67
NCR211	34	5.38	15.17 ± 0.17
NCR247	24	10.15	32.92 ± 0.58

The Frequency and Sequence Diversity of *hrrP* Genes in Nature. The marked increase in overall bacterial fitness of *hrrP*-containing strains and the plasmid-encoded nature of *hrrP* would suggest that *hrrP*-harboring strains may be somewhat abundant in the environment. A PCR-based screen of 150 *Sinorhizobium* isolates from our collection indicates that ∼20% of natural isolates harbor *hrrP* homologs, all of which appear to be encoded on large accessory plasmids. Analysis of a subset of these *hrrP* homologs reveals that they share over 96% identity at the DNA sequence level. Evaluation of an *hrrP* gene tree indicates that *hrrP* phylogeny is discordant with the chromosomal phylogeny of the *Sinorhizobium* strains that harbor them (Fig. 6 and Fig. S6). For example, in several cases, distinct *Sinorhizobium* species harbor nearly identical *hrrP* sequences, but very closely related *Sinorhizobium* strains often harbor relatively divergent *hrrP* alleles.

hrrP may have been introduced into *Sinorhizobium* accessory plasmids relatively recently. The genetic landscape adjacent to *hrrP* has been determined for only two plasmids: the pHR from strain B800 and an accessory plasmid (pSINME01) from *S. meliloti* strain AK83, which is noted for its ineffective nitrogen fixation (16). Despite 97.4% nucleotide sequence identity between these *hrrP* homologs, there is no synteny surrounding the *hrrP* coding region; even the promoter regions are highly divergent (Fig. S7 *A* and *B*). Moreover, both homologs are surrounded by multiple transposable elements that most closely resemble sequences found in the genus *Rhizobium*. Indeed, *hrrP* homologs also are found in various *Rhizobium* species, but in this genus *hrrP* is chromosomally encoded and maintains synteny across different species and strains (Fig. S7*C*). We therefore speculate that *Sinorhizobium* likely acquired *hrrP* from *Rhizobium* via horizontal gene transfer and that *hrrP* has spread among different *Sinorhizobium* genotypes via conjugative- and transposon-mediated processes.

Discussion

Symbiotic compatibility between rhizobia and legumes has been well characterized at the level of early, Nod factor-dependent stages of development (17). This signaling interaction has been appropriately referred to as a "molecular dialogue" (18), but there has been great difficulty in elucidating how that dialogue proceeds into later stages of the symbiosis that encompass the morphological and physiological differentiation of bacteroids. The data presented here are consistent with HrrP providing a means for rhizobia to modulate their own symbiotic developmental fate by directly altering host-derived NCR peptides. The number of NCR peptides thought to be expressed in *M. truncatula* nodules exceeds 590 (19), but the number that have major effects on symbiotic development may be somewhat smaller. The accompanying article (11) reporting the symbiotic essentiality of *M. truncatula* NCR peptide (NCR169) opens the possibility that a rather small ensemble of core NCR peptides may be necessary and sufficient for normal symbiotic development. Therefore a symbiotic modifier such as HrrP may not need to target very many peptides to have a major effect.

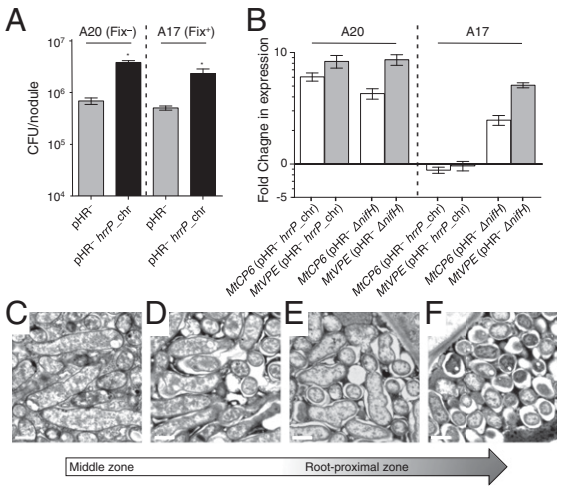

Fig. 5. The effects of *hrrP* on bacterial fitness, senescence, and bacteroid morphology in *M. truncatula* nodules. (*A*) Bacterial fitness for the strains B800 pHR$^-$ (C307) and B800 pHR$^-$ with a chromosomal copy of *hrrP* (PP317), as measured by cfus released from nodules 28 dpi for *M. truncatula* accessions A20 and A17 ($n = 40$ nodules per condition). *$P < 0.05$. (*B*) qRT-PCR analysis of the fold change in expression of the senescence markers *MtCP6* and *MtVPE* for A20 and A17 nodules induced with B800 pHR$^-$ with a chromosomal copy of *hrrP* (PP317) or B800 pHR$^-$ Δ*nifH* (PP411) compared with B800 pHR$^-$ (C307). Error bars in *A* and *B* indicate SEM. (*C*–*F*) Spatial series of transmission electron microscopy images starting at the middle zone and ending at the root-proximal zone of a single *M. truncatula* A20 nodule induced with B800 pHR$^-$ with a chromosomal copy of *hrrP* (PP317). The nodule was harvested at 28 dpi. (Scale bars: 1 μm.)

One of the more interesting properties of *hrrP* is the host and strain dependence of its phenotypic action. These observations imply that genes other than *hrrP*, in both microsymbiont and host, modulate symbiotic compatibility at late developmental stages. For example, hosts may vary in their deployment of NCR peptide arsenals, and rhizobial strains can have varying intrinsic sensitivities to NCR peptides. This idea is supported by the hypervariability of NCR gene sequences across *M. truncatula* accessions (7) and the clear demonstration that at least one *Sinorhizobium* gene, *bacA*, can modulate NCR peptide susceptibility (7, 10). Therefore, the ultimate symbiotic outcome for a given host–strain pair will depend on the interplay between NCR dosage and the bacterial response; *hrrP* may have the effect of shifting the outcome in favor of bacterial insensitivity to NCR peptides.

The symbiosis between rhizobia and legumes is traditionally thought of as a mutualism, but our characterization of HrrP shows that each partner is able to evolve traits that maximize its own benefit from the partnership. Recall that in the nodules of *M. truncatula* A17, *hrrP* does not inhibit nitrogen fixation significantly, but it still increases rhizobial fitness by 4.5-fold (Fig. 5*A*). In natural settings, *hrrP* probably provides an accessory function to *Sinorhizobium* strains that does not detract largely from the benefit they provide their hosts but that substantially increases the ability of bacterial cells to regain proliferative competency after symbiotic services have been rendered. In agricultural settings, however, the pairing of crop plants with genetically incongruous soil microbes may set the stage for synthetic symbiotic incompatibilities such as the one we have dissected here. Exploitative rhizobia in these settings tend to outcompete "superior" inoculant strains for nodule occupancy, as has been reported repeatedly (20, 21). Our data show how readily a single gene such as *hrrP* might contribute to the suppression of nitrogen fixation and how the movement of such a gene on a mobile plasmid could corrupt otherwise superior rhizobium inoculants.

Materials and Methods

Bacterial Strains, Plant Lines, and Culture Conditions. Specific strains and plant lines are listed in Tables S2 and S3, respectively. *Escherichia coli*, *S. meliloti*, and *Agrobacterium tumefaciens* cultures were grown at 37 °C, 30 °C, and 30 °C, respectively, in LB or on LB agar plates with the appropriate antibiotics. For details, see *Supporting Information*.

Plasmid and Strain Construction. Strains, plasmids, NCR peptides, and oligonucleotides are listed in Tables S2 and S4–S6, respectively. Plasmids were constructed using standard molecular techniques. For details, see *Supporting Information*. Plasmid mobilization between strains was mediated via triparental matings with the helper *E. coli* B001 (DH5α harboring pRK600) followed by selection with the appropriate antibiotics.

Construction and Screening of the Plasmid-Specific Transposon Mutant Library. The plasmid-specific transposon library was generated using a mating-out procedure as described in Fig. S1. Transposon insertion sites were mapped onto pHRB800 using arbitrary-PCR for mutant strains that yielded a Fix$^+$ phenotype and maintained pHRB800. More specific details of the protocol are included in *Supporting Information*.

Plant Growth and Nodulation. *M. truncatula* plants were grown in a 4:1 Turface:Vermiculite mixture (Turface Athletics; Thermo-O-Rock West Inc.). Seedlings were inoculated with *Sinorhizobium* 4 d after planting and then were grown under nitrogen-limiting conditions as indicated for individual experiments. For details, see *Supporting Information*. For plant dry weights, samples were placed in an oven at 60 °C for 48 h and then were weighed on an analytical balance. To determine cfus per nodule, nodules were surface sterilized, crushed, serially diluted, and plated on LB agar. The Student's *t* test was used to compare differences between samples.

Acetylene Reduction Assays. Plants were harvested at 21 dpi. Three whole plants were placed in sealed test tubes containing a 10% total atmosphere of acetylene. Plants were incubated for ~12 h, and relative ethylene levels were measured using an Agilent 6890N gas chromatograph (Agilent Technologies, Inc.) For details, see *Supporting Information*.

GUS Staining. 5-Bromo-4-chloro-1*H*-indol-3-yl β-D-glucopyranosiduronic acid (X-GLUC) was used for *in planta* visualization of GUS expression in 10-d-old *M. truncatula* A20 and A17 nodules. p-Nitrophenyl-β-D-glucuronide (PNPG) was used to measure in vitro GUS expression in free-living cells. For details, see *Supporting Information*.

HrrP Modeling, Purification, and Proteolysis Assays. HrrP structural model predictions were generated using iTASSER online (22), and electrostatic modeling predictions were generated using University of California, San Francisco

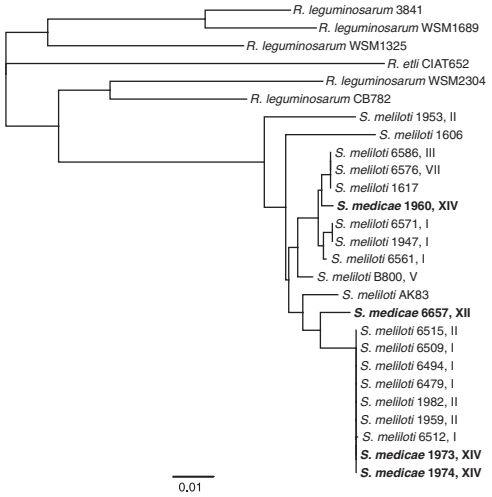

Fig. 6. Sequence diversity of natural *hrrP* alleles. Neighbor-joining phylogenetic tree constructed using DNA sequences for a subset of sequenced *hrrP* homologs identified in the USDA *Sinorhizobium* collection and GenBank for the genera *Rhizobium* and *Sinorhizobium*. To help visualize the lack of concordance between the *hrrP* phylogeny and *Sinorhizobium* phylogeny, we assigned *Sinorhizobium* clades (I–XVI) based on the chromosomal phylogeny reported by Van Berkum et al. (24).

(UCSF) Chimera (23). Overexpressed His_{6x}-tagged HrrP was purified from NiCO21 (DE3) *E. coli* cells (New England Biolabs). NCR peptides were purchased from GenScript or were produced using solid-phase peptide synthesis. HrrP-specific activity was determined by the decrease in the amount of residual substrate compared with HrrP (E62A) matched controls as analyzed via HPLC. HrrP activity also was visualized on Tris-Tricine SDS/PAGE gels. For details, see *Supporting Information*.

RNA Extraction and Quantitative Real-Time PCR Analysis. Total RNA was extracted from *M. truncatula* A17 and A20 nodules, and cDNA pools were synthesized using standard techniques. Quantitative real-time PCR (qRT-PCR) analyses for *MtCP6* and *MtVPE* were performed as described by Pierre et al. (15) using the constitutively expressed *MtC27* and *MtA39* genes as endogenous controls.

Transmission Electron Microscopy. At 28 dpi, whole nodules were excised, fixed, stained, and embedded in Spurr's resin. An ultramicrotome was used to generate the 80-nm sections that then were imaged using a Tecnai G2 T-12 transmission electron microscope. For details, see *Supporting Information*.

Identification of hrrP-Harboring Strains and Phylogenic Tree Assembly. *hrrP* homologs were identified and sequenced from the US Department of Agriculture (USDA) *Sinorhizobium* strain collection or were retrieved from GenBank. For details, see *Supporting Information*. The *hrrP* ORF was used to generate a neighbor-joining phylogenic tree. Clades I–XVI were assigned based on the chromosomal phylogeny reported by Van Berkum et al. (24) at a linkage distance of 0.35.

ACKNOWLEDGMENTS. We thank Michael Standing for technical assistance with the electron microscopy, P. Van Berkum [US Department of Agriculture (USDA) Agricultural Research Service] for providing many of the strains used in this study, and the Biological Resources Centre for *Medicago truncatula* for providing the *M. truncatula* accessions used in this study. Structural graphics and analyses were performed with the University of California, San Francisco (UCSF) Chimera package developed by the Resource for Biocomputing, Visualization, and Informatics at UCSF (supported by National Institute of General Medical Sciences Grant P41-GM103311). This work was funded by National Science Foundation Grant IOS-1054980 and USDA/National Institute of Food and Agriculture Grant 2015-67013-22915 (to J.S.G.). This work was supported in part by National Institutes of Health Grant GM31010 (to G.C.W.); G.C.W. is an American Cancer Society Professor. M.S. is supported by Human Frontier Science Program LT000852/2012.

1. Jones KM, Kobayashi H, Davies BW, Taga ME, Walker GC (2007) How rhizobial symbionts invade plants: The *Sinorhizobium-Medicago* model. *Nat Rev Microbiol* 5(8): 619–633.
2. Mergaert P, et al. (2006) Eukaryotic control on bacterial cell cycle and differentiation in the *Rhizobium*-legume symbiosis. *Proc Natl Acad Sci USA* 103(13):5230–5235.
3. Mergaert P, et al. (2003) A novel family in *Medicago truncatula* consisting of more than 300 nodule-specific genes coding for small, secreted polypeptides with conserved cysteine motifs. *Plant Physiol* 132(1):161–173.
4. Wang D, et al. (2010) A nodule-specific protein secretory pathway required for nitrogen-fixing symbiosis. *Science* 327(5969):1126–1129.
5. Van de Velde W, et al. (2010) Plant peptides govern terminal differentiation of bacteria in symbiosis. *Science* 327(5969):1122–1126.
6. Maunoury N, et al. (2010) Differentiation of symbiotic cells and endosymbionts in *Medicago truncatula* nodulation are coupled to two transcriptome-switches. *PLoS ONE* 5(3):e9519.
7. Nallu S, Silverstein KAT, Zhou P, Young ND, VandenBosch KA (2014) Patterns of divergence of a large family of nodule cysteine-rich peptides in accessions of *Medicago truncatula*. Plant J 78(4):697–705.
8. Penterman J, et al. (2014) Host plant peptides elicit a transcriptional response to control the *Sinorhizobium meliloti* cell cycle during symbiosis. *Proc Natl Acad Sci USA* 111(9):3561–3566.
9. Kondorosi E, Mergaert P, Kereszt A (2013) A paradigm for endosymbiotic life: Cell differentiation of *Rhizobium* bacteria provoked by host plant factors. *Annu Rev Microbiol* 67:611–628.
10. Haag AF, et al. (2011) Protection of *Sinorhizobium* against host cysteine-rich antimicrobial peptides is critical for symbiosis. *PLoS Biol* 9(10):e1001169.
11. Horváth B, et al. (2015) Loss of the nodule-specific cysteine rich peptide, NCR169 abolishes symbiotic nitrogen fixation in the *Medicago truncatula dnf7* mutant. *Proc Natl Acad Sci USA*, 10.1073/pnas.1500777112.
12. Crook MB, et al. (2012) Rhizobial plasmids that cause impaired symbiotic nitrogen fixation and enhanced host invasion. *Mol Plant Microbe Interact* 25(8):1026–1033.
13. Capela D, Filipe C, Bobik C, Batut J, Bruand C (2006) *Sinorhizobium meliloti* differentiation during symbiosis with alfalfa: A transcriptomic dissection. *Mol Plant Microbe Interact* 19(4):363–372.
14. Shen Y, Joachimiak A, Rosner MR, Tang W-J (2006) Structures of human insulin-degrading enzyme reveal a new substrate recognition mechanism. *Nature* 443(7113):870–874.
15. Pierre O, et al. (2014) Involvement of papain and legumain proteinase in the senescence process of *Medicago truncatula* nodules. *New Phytol* 202(3):849–863.
16. Galardini M, et al. (2011) Exploring the symbiotic pangenome of the nitrogen-fixing bacterium *Sinorhizobium meliloti*. *BMC Genomics* 12:235–249.
17. Long SR (1996) Rhizobium symbiosis: Nod factors in perspective. *Plant Cell* 8(10): 1885–1898.
18. Denarie J, Debelle F, Truchet G, Prome J (1993) Rhizobium and legume nodulation: A molecular dialogue. *New Horizons in Nitrogen Fixation*, Current Plant Science and Biotechnology in Agriculture, eds Palacios R, Mora J, Newton WE (Springer, Dordrecht, The Netherlands), Vol 17, pp 19–30.
19. Young ND, et al. (2011) The *Medicago* genome provides insight into the evolution of rhizobial symbioses. *Nature* 480(7378):520–524.
20. Streeter J (1994) Failure of inoculant rhizobia to overcome the dominance of indigenous strains for nodule formation. *Can J Microbiol* 40(7):513–522.
21. Vlassak K, Vanderleyden J, Graham P (1997) Factors influencing nodule occupancy by inoculant rhizobia. *Crit Rev Plant Sci* 16:163–229.
22. Yang J, et al. (2015) The I-TASSER Suite: Protein structure and function prediction. *Nat Methods* 12(1):7–8.
23. Pettersen EF, et al. (2004) UCSF Chimera—a visualization system for exploratory research and analysis. *J Comput Chem* 25(13):1605–1612.
24. van Berkum P, Elia P, Eardly BD (2006) Multilocus sequence typing as an approach for population analysis of *Medicago*-nodulating rhizobia. *J Bacteriol* 188(15):5570–5577.
25. Griffitts JS, Long SR (2008) A symbiotic mutant of *Sinorhizobium meliloti* reveals a novel genetic pathway involving succinoglycan biosynthetic functions. *Mol Microbiol* 67(6):1292–1306.
26. Price PA, Jin J, Goldman WE (2012) Pulmonary infection by *Yersinia pestis* rapidly establishes a permissive environment for microbial proliferation. *Proc Natl Acad Sci USA* 109(8):3083–3088.
27. Quandt J, Hynes MF (1993) Versatile suicide vectors which allow direct selection for gene replacement in gram-negative bacteria. *Gene* 127(1):15–21.
28. Wells DH, Long SR (2002) The *Sinorhizobium meliloti* stringent response affects multiple aspects of symbiosis. *Mol Microbiol* 43(5):1115–1127.